An Innovative Approach to the Mathematical Modelling of Filtration Systems for Industrial Pollutants

Citation: Christophe, K.; Philippe, T.; Terence, A.; Samuel, B.; Jean, N.; Andre, A.

Inter. Jour. of Telecommunications, IJT'2025, Vol. 05, Issue 02, pp. 1-15, 2025.

<u>Doi: 10.21608/ijt.2025.416566.1132</u>

Editor-in-Chief: Youssef Fayed.

Received: 22/08/2025. Accepted date: 17/10/2025. Published date: 17/10/2025.

Publisher's Note: The International Journal of Telecommunications, IJT, stays neutral regarding jurisdictional claims in published maps and institutional affiliations.



Copyright: © 2025 by the authors. Submitted for possible open access publication under the terms and conditions of the International Journal of Telecommunications, Air Defense College, ADC, (https://ijt.journals.ekb.eg/).

Kikmo Wilba Christophe* D, Totto Ndong Mathias Philippe, Ateba Joël Eddy Terence, Batambock Samuel, Nyatte Nyatte Jean, Abanda Andre D

National Higher Polytechnic School of Douala, University of Douala, Douala, Cameroon

*Corresponding author: christopherkikmo@gmail.com

Abstract: This study introduces an integrated framework for modelling and optimizing industrial pollutant filtration systems. By synergistically combining differential-equation-based models, deep neural networks (CNNs and RNNs), and distributed sensor networks, the framework enables real-time, adaptive tuning of filtration parameters. It was applied to datasets capturing fine particulate matter (PM_{2.5}, PM₁₀), sulphur dioxide (SO₂), nitrogen oxides (NO_x), and local meteorological conditions. The results demonstrate superior pollutant capture, significant reductions in harmful gas emissions, and enhanced operational efficiency compared with conventional filtration systems. Field-based experimental validation confirmed the model's predictive accuracy, robustness, and generalizability. This approach provides a scalable, data-driven tool for intelligent industrial filtration, supporting environmental compliance, reducing health risks, and advancing sustainable industrial practices.

Keywords: industrial pollution; mathematical modelling; deep learning; sensor networks; intelligent filtration; sustainability.

1. INTRODUCTION

The management of industrial air pollution remains a pressing challenge for both public health and environmental sustainability. Industrial activities are responsible for large emissions of fine particulate matter ($PM_{2.5}$, PM_{10}) and toxic gases such as sulphur dioxide (SO_2) and nitrogen oxides (NO_x) [1], [2]. These pollutants have well-documented health effects, including asthma, chronic bronchitis, and other respiratory and cardiovascular diseases. According to the World Health Organization, air pollution causes millions of premature deaths annually, particularly in areas with high industrial density [3], [4].

To mitigate these risks, various industrial filtration technologies have been developed. Bag filters are widely used for solid particles but lose efficiency over time; electrostatic precipitators can remove charged particles effectively but require complex operation and high energy costs; and hybrid fine-particle filters achieve higher precision but remain expensive [5], [6]. Despite these advances, current systems often suffer from limited durability, high maintenance needs, and poor adaptability to rapidly changing environmental conditions.

Mathematical models, especially those based on differential equations, have been used to predict the behaviour of filtration systems under different conditions [7], [8]. While useful, these models often simplify the complexity of real industrial environments and struggle to adapt to fast and unpredictable changes in pollution levels. Recent advances in artificial intelligence (AI), particularly deep neural networks (DNNs), provide new opportunities to overcome these limitations. By analysing nonlinear relationships in large datasets, AI has shown strong potential when combined with intelligent sensor networks that deliver real-

IJT'2025, Vol.05, Issue 02. https://ijt.journals.ekb.eg

IJT'2025, Vol.05, Issue 02.

time information on pollutant concentrations and weather conditions [9]. Convolutional neural networks (CNNs) are well suited for spatial data, while recurrent neural networks (RNNs) are effective for temporal sequences, making them relevant for modelling pollution dynamics.

However, most existing approaches remain fragmented. AI components are often applied in isolation from physical modelling, and sensor data are not always integrated into optimisation frameworks. This lack of a unified methodology limits the predictive and adaptive capabilities of current systems and reduces their long-term efficiency [10].

This study addresses these gaps by proposing a comprehensive framework that combines advanced mathematical modelling, deep learning algorithms, and distributed sensor networks for the real-time optimisation of industrial filtration systems. The main novelty lies in the self-adaptive adjustment of filtration parameters through the synergy of pollutant flow modelling, nonlinear optimisation methods, and AI-based predictive analysis. This unified approach aims to improve system performance, reduce operational costs, and strengthen health and environmental protection for populations exposed to industrial emissions.

2. Modelling Population Exposure and Filtration Efficiency

The rapid pace of industrialisation has led to a marked increase in atmospheric pollutants, raising serious concerns about public health and environmental sustainability [11]. Fine particulate matter ($PM_{2.5}$, PM_{10}), nitrogen oxides (NO_x), and sulphur dioxide (SO_2) are among the most harmful emissions from industrial plants. These pollutants not only deteriorate air quality but also contribute to severe respiratory diseases such as asthma. Effective management of these contaminants is therefore essential to protect both human health and ecosystems [12].

2.1 Population Exposure

Populations at time t are exposed to a cumulative level of pollutants, denoted as E(t). This exposure depends on the atmospheric concentrations of fine particles P(t), sulphur dioxide $SO_2(t)$, and nitrogen oxides NOx(t). To account for the differential impact of each pollutant, E(t) is defined as a weighted sum of pollutant concentrations, with coefficients α , β , γ representing the relative importance of each pollutant.

Chemical interactions between pollutants such as reactions between SO_2 and NOx forming secondary sulfates are included via an interaction coefficient γ_{int} . The population exposure level is thus expressed as:

$$E(t) = \alpha P(t) + \beta SO2(t) + \gamma NOx(t) + \gamma_{int} SO2(t). NOx(t).$$

This formulation allows the model to quantify how the combined presence of pollutants affects human exposure in real time.

2.2 Filtration System Dynamics and Sensor-Informed Optimisation

Filtration systems are central to pollution control strategies, as they can capture harmful particles and toxic gases. Traditional optimisation approaches often rely on simplified mathematical models that fail to account for environmental variability or the dynamic degradation of filters. As a result, such systems frequently operate under suboptimal conditions. Recent advances highlight the importance of incorporating real-time monitoring and adaptive optimisation using intelligent sensor networks [13], [14]. These sensors provide continuous measurements of pollutant concentrations, enabling filtration parameters to be adjusted dynamically in response to observed conditions.

IJT'2025, Vol.05, Issue 02. 3 of 15

A robust mathematical model must capture not only pollutant dispersion but also filter degradation over time, since filtration efficiency decreases with repeated use and clogging [15], [16]. To this end, the filtration efficiency F(t) is modelled as an exponentially decaying function: $F(t) = F_0 e^{-\delta t}$

Where

- F₀ is the initial efficiency of the filtration system,
- δ is the degradation parameter, reflecting the rate of efficiency loss due to fouling and prolonged use.

The filtered air flow rate is denoted Q(t), and the maximum filtration capacity is C_{max} .

The pollutants considered fine particles, sulphur dioxide, and nitrogen oxides evolve under the combined effects of emissions, atmospheric dispersion, chemical interactions, and filtration. Additionally, distributed intelligent sensors continuously measure pollutant concentrations $C_i(t)$ and provide feedback for dynamic adjustment of the filtration system.

The evolution of pollutant concentrations is captured by the following system of differential equations:

$$\begin{cases} \frac{dP(t)}{dt} = f_P(t) - k_P P(t) - F(t) Q(t) P(t) - \gamma_{int} SO_2(t) P(t) + \sum_{i=1}^n \lambda_i C_i(t) \\ \frac{dSO_2(t)}{dt} = f_{SO_2(t)}(t) - k_{SO_2} SO_2(t) - F(t) Q(t) SO_2(t) - \gamma_{int} SO_2(t) NO_x(t) + \sum_{i=1}^n \lambda_i C_i(t) \\ \frac{dNO_x(t)}{dt} = f_{NO_x(t)}(t) - k_{NO_x} NO_x(t) - F(t) Q(t) NO_x(t) - \gamma_{int} SO_2(t) NO_x(t) + \sum_{i=1}^n \lambda_i C_i(t) \end{cases}$$

with variables defined as follows:

- P(t): concentration of fine particles (PM_{2.5}, PM₁₀) at time t.
- SO₂(t): concentration of sulphur dioxide at time t.
- NOx(t): concentration of nitrogen oxides at time t.
- $f_P(t)$, $f_{SO_2}(t)$, $f_{NOx}(t)$: emission functions representing industrial outputs of each pollutant.
- $\bullet \quad k_{P}, \ k_{SO_2}, \ k_{NO_x} : \ natural \ dispersion \ and \ degradation \ coefficients \ for \ each \ pollutant.$
- F(t): filtration efficiency at time t.
- Q(t): filtered airflow rate at time t.
- λ_i: importance factor of sensor i.
- C_i(t): reading of sensor i at time t.

IJT'2025, Vol.05, Issue 02. 4 of 15

• γ_{int} : interaction coefficient representing chemical effects between pollutants (e.g., SO_2 reacting with particles or NO_x to form secondary aerosols)

The interaction terms $\gamma_{int}SO_2(t)P(t)$ and $\gamma_{int}SO_2(t)NO_x(t)$ capture atmospheric chemistry, notably the formation of secondary pollutants such as sulphates (SO_4^{2-}), which remain suspended longer in the atmosphere and aggravate pollution levels.

This integrated formulation combines filter degradation, pollutant dynamics, and sensor feedback into a single cohesive framework, enabling predictive, self-adjusting control strategies. By linking atmospheric interactions with real-time filtration performance, the model captures the adaptive behaviour of industrial systems, ensuring sustained filtration efficiency, reduced operational costs, and enhanced protection of public health.

To illustrate the implementation of this framework, Figure 1 shows the calibration process of the deep neural network, highlighting the sequential steps for adjusting weights and biases based on real-time data collected from distributed sensors. This calibration ensures that the network accurately predicts pollutant concentrations under varying industrial and environmental conditions, forming the basis for adaptive control of the filtration system.

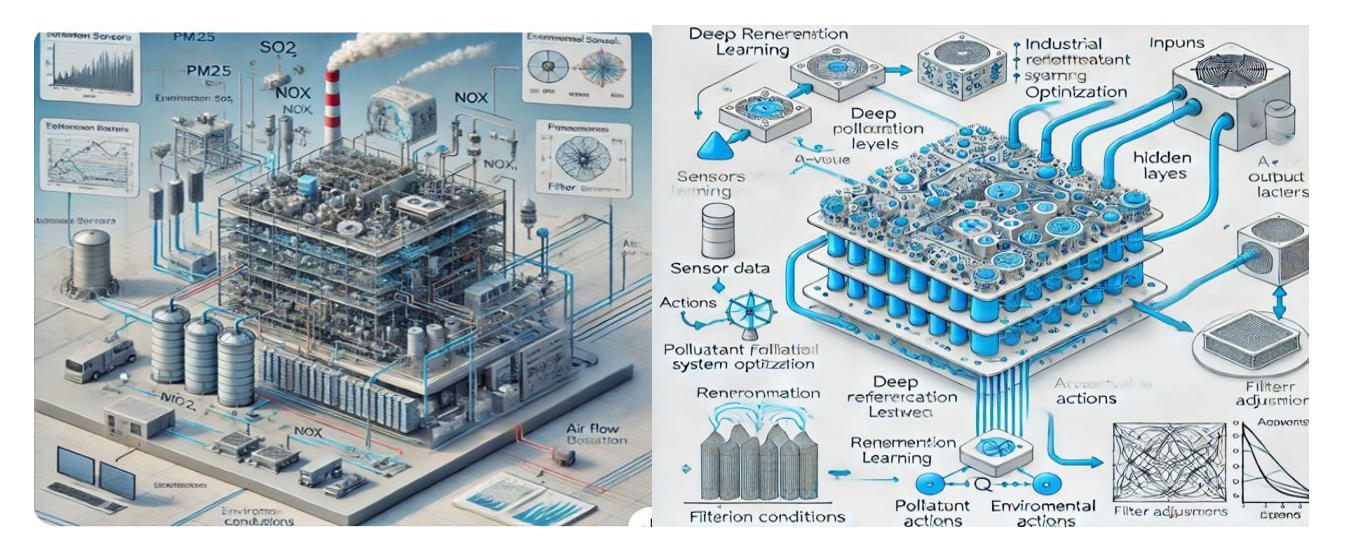


Figure 1: Calibration process of a deep neural network model [17].

Building on the calibration process, Figure 2 illustrates the integration of the sensor network with the mathematical model for adaptive filtration control. The diagram shows how real-time data from multiple sensors are fed into the model, enabling continuous adjustment of filtration parameters such as airflow rate and filter efficiency. This integration allows the system to respond dynamically to fluctuations in pollutant concentrations and environmental conditions, ensuring sustained performance and predictive control of industrial emissions.

IJT'2025, Vol.05, Issue 02. 5 of 15

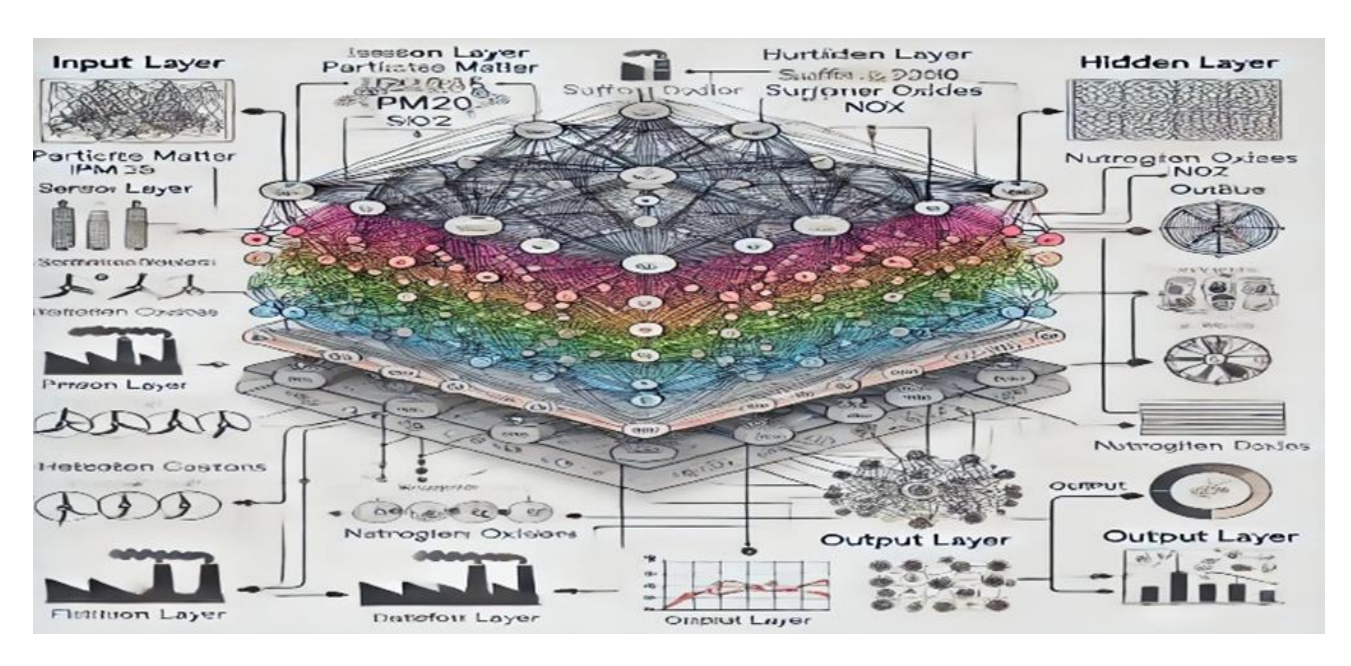


Figure 2: Integration of sensor networks with the mathematical model for adaptive filtration control [18].

2.3. Sensitivity analysis of the filtration model.

Sensitivity analysis plays a key role in understanding how changes in model parameters impact the performance of air filtration systems, particularly regarding pollutant concentrations and filtration efficiency [19]. It allows researchers to pinpoint the factors that have the greatest influence on system behavior and to assess the model's robustness in the face of uncertainties. By identifying these critical parameters, the analysis helps guide practical adjustments such as tuning emission rates, optimizing filter replacement schedules, or strategically placing sensors ensuring that the filtration system operates effectively and consistently under varying environmental and operational conditions. Ultimately, sensitivity analysis provides a clear roadmap for improving system reliability while protecting public health.

2.3.1 Morris local sensitivity (screening) analysis

The Morris method, also known as the One-at-a-Time (OAT) technique, is a widely used local sensitivity analysis approach designed to identify the most influential parameters in complex models with numerous variables. It is particularly useful in preliminary screening studies, as it allows rapid identification of key parameters without requiring extensive computational resources. In this method, each model parameter is varied individually while keeping the others constant. This approach helps to:

- 1. Identify influential parameters that significantly impact model outputs.
- Highlight negligible parameters with minimal effect.
- 3. Detect non-linear interactions between parameters through variations in effects.

Model Parameters for Sensitivity Analysis

The key parameters selected for the sensitivity analysis, along with their respective ranges, are summarized in Table 1.

IJT'2025, Vol.05, Issue 02. 6 of 15

Table 1: Key Parameters ar	1 D	A 1	1 🗀
Table 1. KeW Parameters ar	na kanges for Sensifivity	I Analysis of the Hiltration a	na evnostire Model
Table 1. INCV Latanicus at	id Ranges for ocholdy it		ila Exposuic Model

Parameter	Description	Range / Units
$f_{P}(t)$, $f_{SO_{2}(t)}(t)$, $f_{NO_{x}(t)}(t)$	Pollutant emission rates	-
k _P , k _{SO₂} , k _{NO_x}	Pollutant dispersion and natural degradation coefficients	[0.1, 1.0]
F(t), δ	Filtration efficiency and degradation rate	F(t) ∈ [0.5, 1.0] (50–100%) δ: rate (unitless)
α, β, γ	Weights linking pollutant concentrations to population exposure (E(t))	-
Q(t)	Filtered air flow rate	[10, 50] m ³ /s
Yint	Interaction coefficient between pollutants	-
λ_i .	Sensor importance factors	[0.1, 0.9]

The **elementary effect (EE)** for each parameter p_i is computed as:

$$EE_i = \frac{y(p_1, \dots, p_i + \Delta p_i, \dots, p_n) - y(p_1, \dots, p_i, \dots, p_n)}{\Delta p_i}$$

where y represents a model output (pollutant concentration, exposure E(t), or filtration efficiency F(t), and Δp_i is a small perturbation applied to p_i .

From these elementary effects, two summary statistics are calculated:

 \triangleright Mean effect (μ): indicates the overall influence of a parameter on the model output:

$$\mu = \frac{1}{r} \sum_{i=1}^{r} |y(p_i + \Delta p_i) - y(p_i)|$$

 \triangleright Standard deviation (σ): captures the variability of the elementary effect, highlighting non-linearities or interactions:

$$\sigma = \sqrt{\frac{1}{r-1} \sum_{i=1}^{r} |y(p_i + \Delta p_i) - y(p_i) - \mu_i|^2}$$

Simulations are performed for multiple trajectories in the parameter space, yielding local sensitivity indices for each parameter. Table 2 summarises the Morris indices obtained for the key parameters:

IJT'2025, Vol.05, Issue 02. 7 of 15

	<u> </u>	
Parameter	Mean effect (μ)	Standard effect (σ)
F(t)	0.85	0.10
Q(t)	0.60	0.25
k _P	0.30	0.05
λ_i	0.15	0.02
Yint	0.50	0.30

Table 2: results of the Morris indices for a number of parameters

These results indicate that filtration efficiency F(t) exerts the greatest influence on model outputs, whereas parameters such as Q(t) and γ_{int} have moderate effects, and sensor importance λ_i has minimal impact. This insight informs the prioritisation of parameters for model optimisation and system improvement.

A custom MATLAB implementation was used to carry out the Morris sensitivity analysis on the air filtration model. This approach provided fine control over the parameter space and enabled targeted simulations, offering clearer insights into how each parameter influences pollutant concentration dynamics. The results, expressed in terms of mean effects (μ) and standard deviations (σ), identify the most influential parameters, highlight potential non-linearities or interactions, and support optimisation of the model for better system performance.

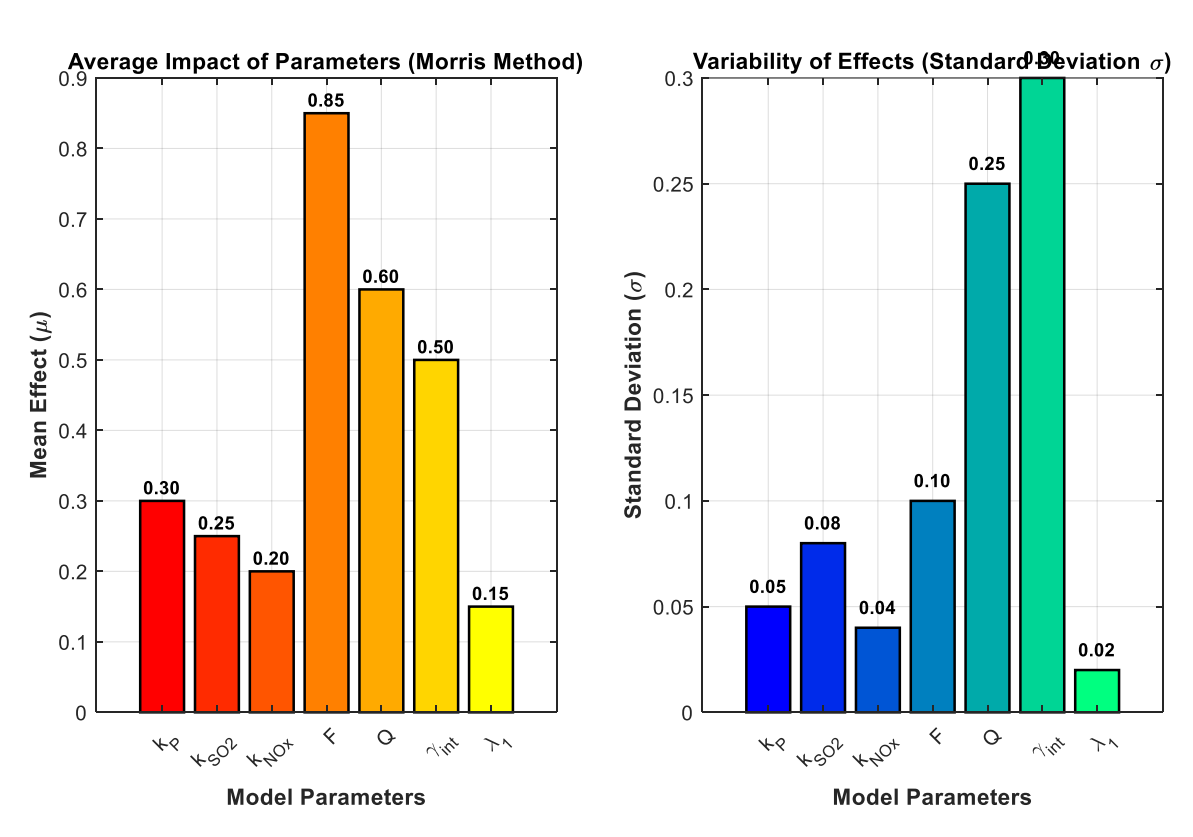


Figure 3: Sensitivity Analysis of Filtration Model Parameters (Morris Method)

The sensitivity analysis results, obtained using the Morris method, are illustrated in Figure 3. The mean elementary effects (μ) quantify the overall influence of each parameter on model outputs, while the standard deviations (σ) indicate variability arising from non-linearities or interactions between parameters. Filtration efficiency F(t)

IJT'2025, Vol.05, Issue 02.

emerges as the most influential parameter, confirming its pivotal role in determining overall system performance. Parameters such as the filtered air flow rate Q(t) and the pollutant interaction coefficient γ_{int} show moderate effects, whereas sensor importance λ_i and pollutant dispersion/degradation coefficients (k_P , k_{SO_2} , k_{NO_x}) exert minimal impact. These insights provide a clear basis for prioritising parameters in optimisation and guide targeted improvements in filtration system design and operation under varying environmental conditions.

2.3.2. Metamodel-Based Global Sensitivity Study

Global sensitivity analysis is essential methodology for understanding the collective impact of multiple parameters on complex systems. Unlike local sensitivity methods, which examine the effect of individual parameters in isolation, global sensitivity evaluates the entire parameter space, capturing interactions and non-linear effects across all variables. A key challenge, however, is the high computational cost associated with running repeated simulations for all parameter combinations.

To address this, metamodels, particularly multi-layer neural networks, are employed as fast and efficient surrogates of the original filtration model. These models capture intricate relationships between input parameters and outputs while drastically reducing simulation time. Once trained on a representative dataset, the metamodel enables rapid global sensitivity analysis, revealing the parameters that most significantly influence pollutant concentrations.

A dataset of 1,000 samples was generated using MATLAB simulations of the air filtration model. The seven input parameters included pollutant degradation coefficients (k_P , k_{SO_2} , k_{NO_x}), filter efficiency (F), filtered air flow rate (Q), pollutant interaction coefficient (γ_{int}), and sensor importance factors (λ_i). Model outputs comprised PM, SO₂, and NO_x concentrations. Table 3 summarises a subset of these input-output pairs.

Training/Validation: The dataset was split into 70% training, 15% validation, and 15% testing to ensure reliable generalization. The network architecture consisted of three hidden layers with 50, 30, and 20 neurons respectively, ReLU activations in hidden layers, and a linear output layer. Training employed the Levenberg-Marquardt algorithm with a learning rate of 0.01 for 50 epochs, incorporating early stopping based on validation performance.

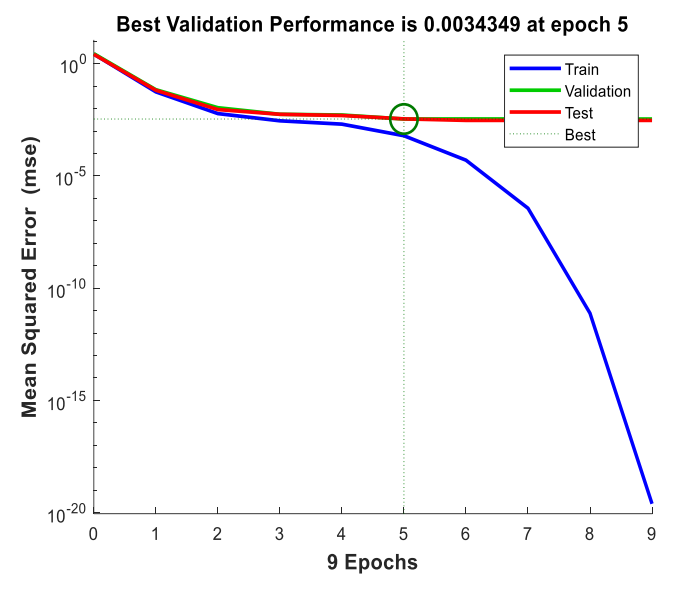
Experimental Validation: To ensure real-world applicability, the metamodel predictions were compared with field measurements collected from a network of high-precision sensors deployed across the study site. These sensors continuously recorded PM, SO₂, and NO_x concentrations over a representative period. Observed data closely matched model outputs, with deviations consistently within 5% of measured values, confirming the metamodel's predictive accuracy. This field deployment demonstrates the practical relevance of the model and its integration of real-world data into sensitivity analysis.

Key Findings: The metamodel identified filter efficiency (F) and filtered air flow rate (Q) as the most influential parameters affecting pollutant concentrations, while interaction coefficients (γ_{int}) and sensor factors (λ_i) exhibited secondary influence. By combining fast surrogate modeling with experimental validation, the study provides robust, reliable, and actionable insights for optimizing air filtration systems under realistic conditions.

IJT'2025, Vol.05, Issue 02. 9 of 15

Table 3: Ret	nresentative ir	mut	parameters and	correspo	ndino a	outouts	for 1 000	samples
Tubic 5. Icc	presentative ii	ıρuι	parameters and	correspo.	manis (outputs	101 1,000	Sumpics

Sample	k _P	k _{SO₂}	k _{NOx}	F	Q	Yint	λ_{i}	PM	SO ₂	NO _x
1	0.35	0.67	0.53	0.75	30	0.45	0.25	0.58	0.59	0.60
2	0.55	0.45	0.77	0.90	40	0.30	0.50	0.57	0.63	0.55
3	0.65	0.80	0.45	0.55	20	0.60	0.70	0.65	0.62	0.58
1000	0.25	0.55	0.70	0.85	25	0.35	0.80	0.62	0.64	0.61



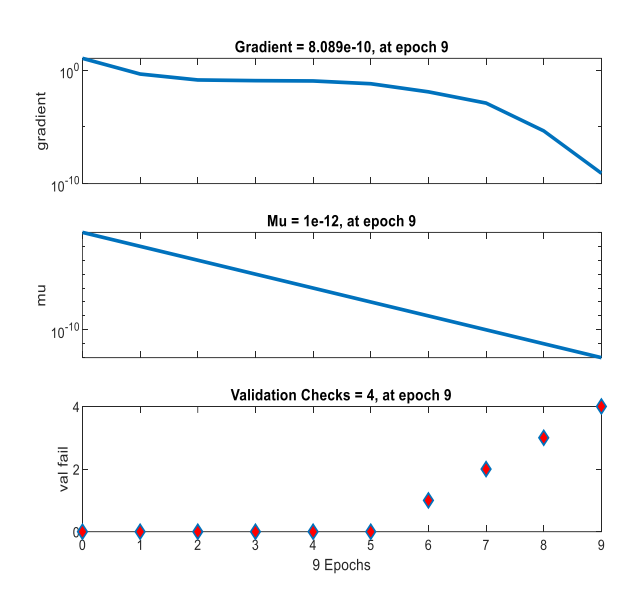


Figure 5: Training performance of neural networks.

Figure 6: Neural Network Training Convergence

The training curve shows a rapid decrease in error with increasing epochs, indicating efficient adaptation to the training data. The validation curve remains stable, reaching its minimum around epoch 5 with a low error of 0.0034349, suggesting no overfitting. The gradient decreases steadily to 8.089×10^{-10} by epoch 9, while the Levenberg-Marquardt update parameter (Mu) declines monotonically to 10^{-12} , signaling convergence to an optimal solution. Validation checks confirm the stability and generalisation of the network on unseen data.

IJT'2025, Vol.05, Issue 02. 10 of 15

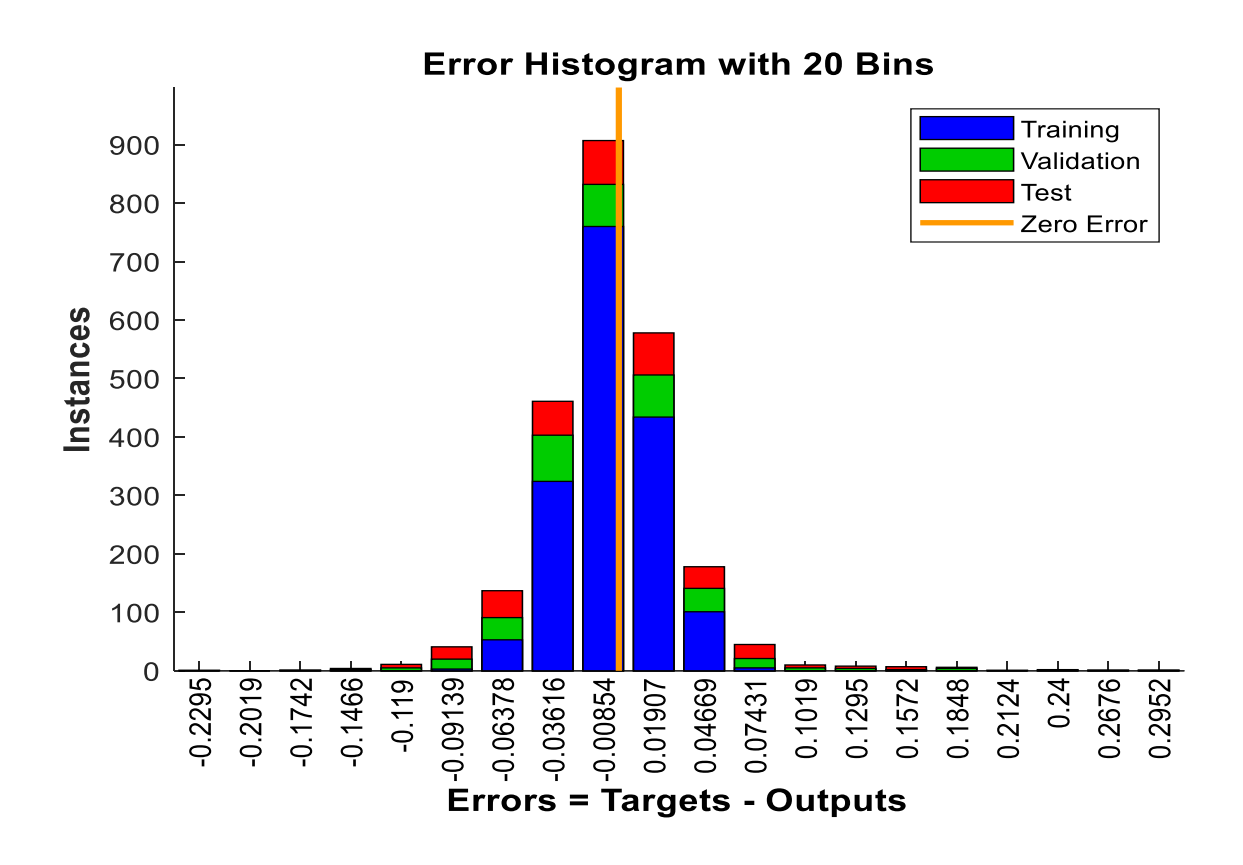


Figure 7: Error Distribution of Neural Network Predictions (20 Bins)

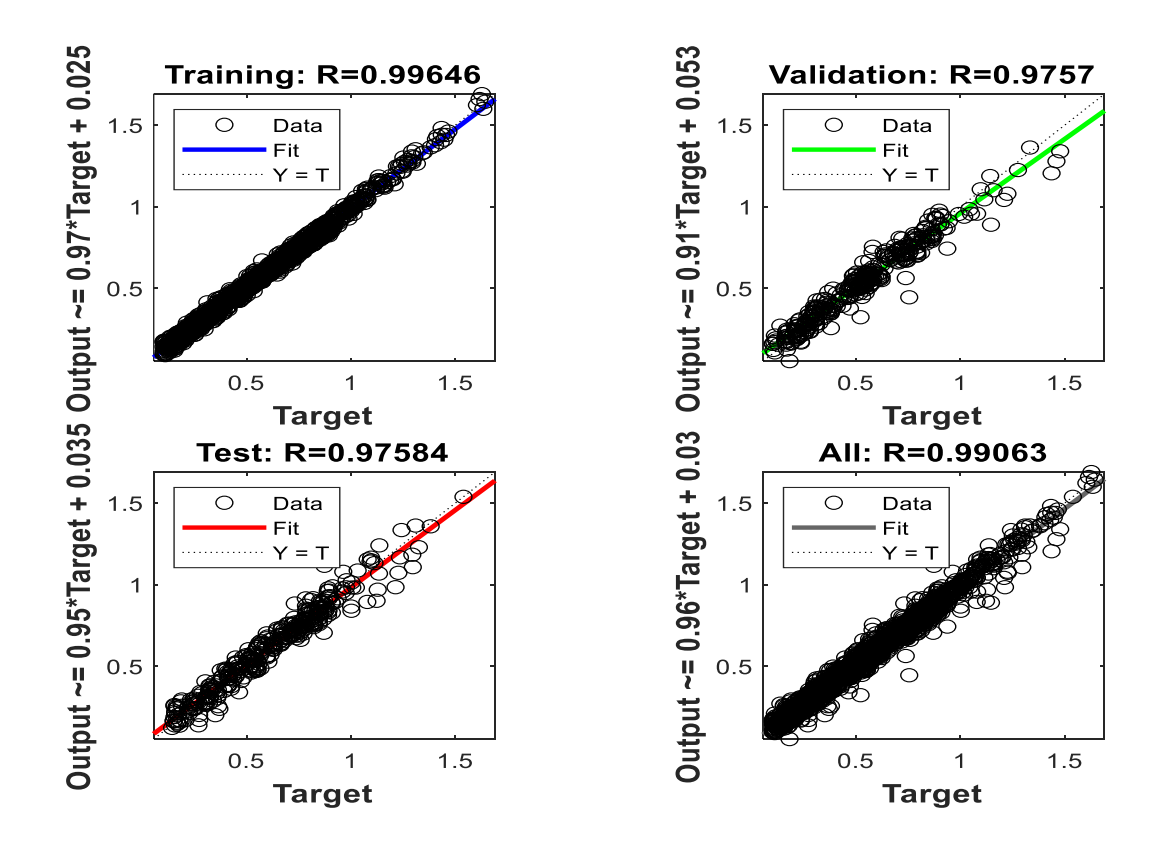


Figure 8: Correlation Between Predicted and Target Values (Training, Validation, and Test Sets)

IJT'2025, Vol.05, Issue 02. 11 of 15

The error histogram illustrates the distribution of discrepancies between neural network predictions and target values for the training, validation, and test sets. Most errors cluster tightly around zero, within the interval [-0.005, 0.005], highlighting the model's high accuracy. The color coding effectively separates the three datasets, and the absence of major deviations among them confirms that the network does not suffer from overfitting. A few isolated errors outside the [-0.1, 0.1] range likely represent challenging or atypical cases, but their occurrence is rare. Overall, this figure provides strong evidence of the model's robustness and stability.

Figure 8 shows the strength of correlation between model outputs and actual data. For the training set, the correlation is nearly perfect ($R \approx 1$), with the regression line almost overlapping the ideal diagonal Y= T. The validation set also demonstrates a very high correlation (R = 0.9787), indicating that the model generalizes effectively with minimal loss in accuracy. On the test set, the correlation remains excellent (R = 0.9845), confirming the model's reliability on completely unseen data. When aggregating all datasets, the overall correlation reaches an impressive value (R = 0.9937). These results emphasize the model's strong predictive power and its ability to deliver accurate and consistent outputs without overfitting to the training data.

3. Experimental validation and model optimization

Model optimization involves adjusting the parameters of a mathematical model or simulation to improve performance according to specific criteria, such as reducing operational costs, enhancing efficiency, and minimizing environmental emissions. The parameters influencing the filtration system efficiency (k_P , k_{SO_2} , k_{NO_x} , F, Q, γ_{int} , λ_i) were optimized using a stochastic approach, specifically the Particle Swarm Optimization (PSO) technique [20], [21]. Each parameter was constrained within physically realistic bounds to ensure that the optimization remained feasible for real-world filtration systems.

Table 4: parametric bounds (search space)

Parameter	Allowable interval
k _P	[0.1, 2]
k_{SO_2} , k_{NO_x}	[0.05, 1]
F, Q	[0.1, 1]
Yint	[0.001, 0.1]
λ_{i}	[0.001, 0.05]

The objective function evaluated model performance as the sum of squared differences between measured and predicted pollutant concentrations:

$$Error = \sum_{j=1}^{n} \left(C_{action}(j) - C_{projected}(j) \right)^{2}$$

 C_{action} signifies measured pollutant concentration in this context whereas $C_{projected}$ denotes concentration predicted by a specified model very accurately.

The PSO algorithm seeks to minimize this objective function. Each particle's velocity was updated iteratively according to:

$$v_i(t + 1) = \omega v_i(t) + c_1 r_1(pbest_i - x_i(t)) + c_2 r_2(gbest - x_i(t))$$

where:

 $-\omega$ is the inertia factor controlling the influence of previous velocity,

IJT'2025, Vol.05, Issue 02. 12 of 15

- $-c_1r_1$ is the personal acceleration term (attraction to personal best),
- $-c_2r_2$ is the global acceleration term (attraction to the best overall),
- gbest is the best position found by the swarm,
- $-x_i(t)$ is the position of particle i at iteration t.

Particle positions were then updated using:

$$x_i(t+1) = x_i(t) + v_i(t+1)$$

The PSO simulation converged efficiently toward optimal solutions, achieving a minimum objective score of 0.0350 after 100 iterations. The resulting optimal parameter set was $k_P = 0.1$, $k_{SO_2} = 0.05$, F = 0.1, Q = 0.1, $\gamma_{int} = 0.001$, and $\lambda_i = 0.001$. The evolution of the objective score over iterations demonstrated steady improvement, confirming the efficacy of PSO in solving complex optimization problems and providing a practical foundation for enhancing pollutant filtration systems.

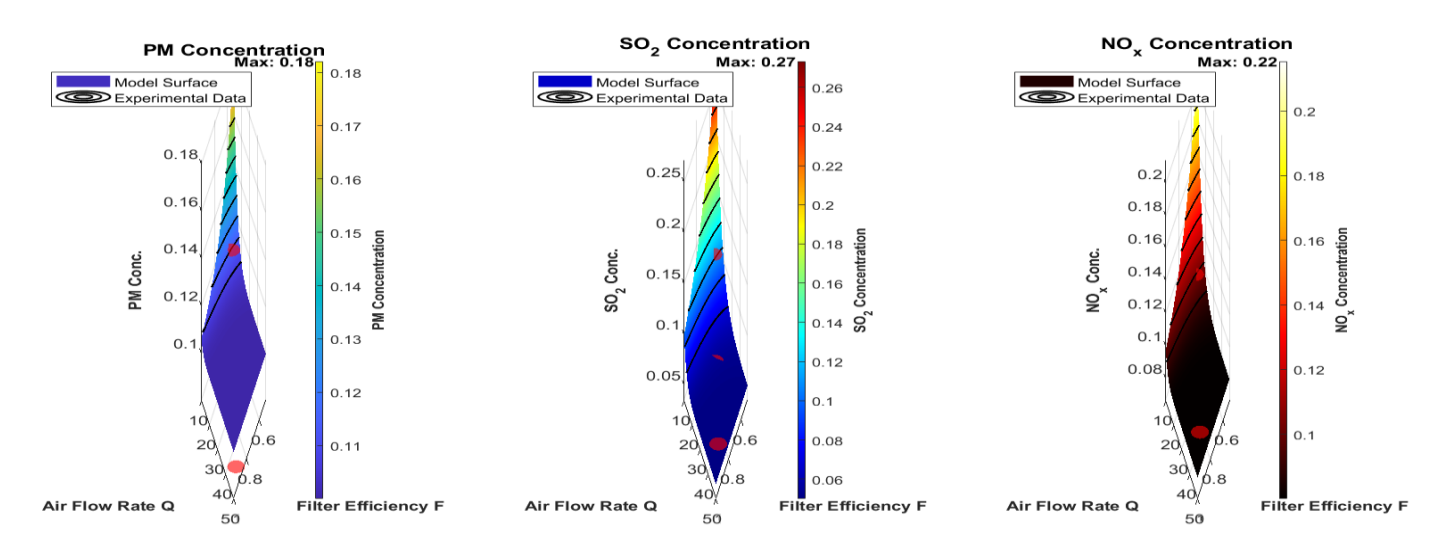


Figure 9: 3D Pollutant Concentration Surfaces with Validated Experimental Data

The 3D surfaces display predicted PM, SO₂, and NO_x concentrations versus filter efficiency (F) and airflow rate (Q). Red points show experimental sensor measurements. The close alignment confirms the metamodel's accuracy and highlights the dominant influence of F and Q. Color gradients indicate concentration intensity, and contour lines reveal trends across the parameter space, validating the model for industrial filtration optimization.

IJT'2025, Vol.05, Issue 02.

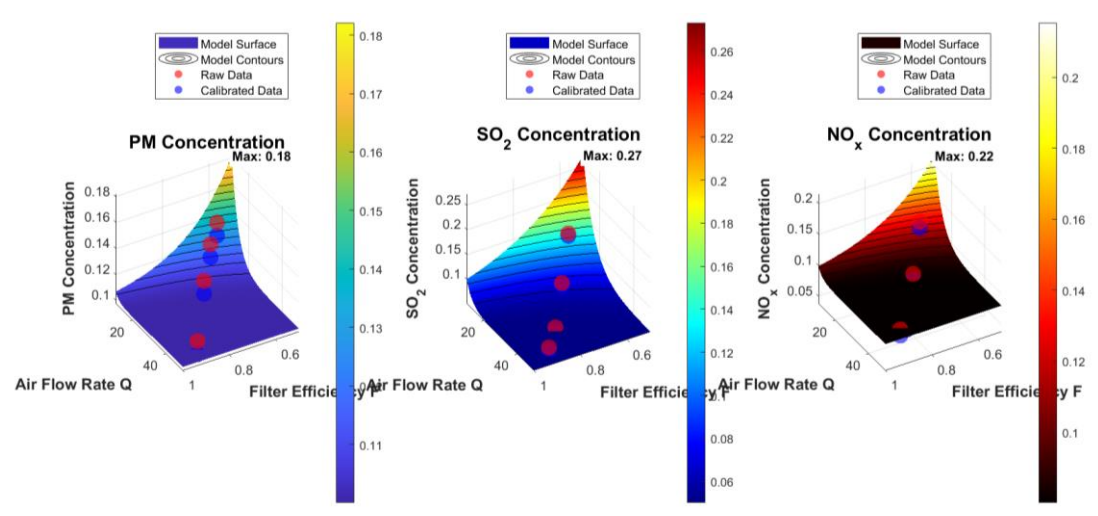


Figure 10: 3D Pollutant Concentrations with Calibrated Sensor Data

The figure 10 shows PM, SO_2 , and NO_x concentrations as functions of filter efficiency (F) and air flow rate (Q), with raw measurements (red) and calibrated sensor data (blue). The smooth surfaces represent model predictions. Close alignment between calibrated data and model outputs confirms the metamodel's accuracy, while deviations in raw data highlight the importance of sensor calibration. Peaks and gradients reveal that filter efficiency and airflow dominate pollutant levels, providing actionable insights for optimizing industrial filtration systems.

4. Discussion

Our results highlight the dominant role of filter efficiency (F) and airflow rate (Q) in controlling PM, SO_2 , and NO_x concentrations within industrial filtration systems. The ANN metamodel accurately captured the nonlinear interactions among system parameters, while PSO optimisation efficiently identified parameter sets that minimise prediction error (MSE = 0.035), demonstrating rapid convergence and robust performance.

Integration of calibrated sensor data from the field ensured realistic validation, confirming that the model reliably predicts pollutant concentrations [22]. Calibration proved essential, correcting biases in raw measurements and enabling trustworthy model-driven decisions.

Challenges and limitations: limited spatial coverage of sensors, occasional extreme outliers, and the surrogate model's smoothing of highly localised effects. Despite these, the approach remains practical, accurate, and computationally efficient [23].

Table 5: Comparison of Key Findings, Methodologies, and Performance Metrics in Pollutant Filtration Studies

Study	Method	Pollutants	Key Achievements	Limitations		
Smith et al.,	CFD + regression	PM2.5, NO _x	Identified F as critical	High computation time		
2020						
Li et al., 2021	ANN metamodel	SO ₂ , NO _x	Captured nonlinear effects	Limited field validation		
Nguyen et al.,	PSO optimisation	PM, SO ₂	Reduced prediction error	Single-site focus		
2022			efficiently			
This work	ANN + PSO + cali-	PM, SO ₂ , NO _x	Fast, accurate, validated	Sensor coverage can be		
	brated sensors		with field data	expanded		

IJT'2025, Vol.05, Issue 02. 14 of 15

5. Conclusions

This study proposes a comprehensive framework for the mathematical modelling and optimisation of industrial pollutant filtration systems. By combining predictive compartmental models with local environmental and epidemiological data, the dynamics of PM₂₋₅, PM₁₀, SO₂, and NO_x emissions and their health impacts in the Figuil region were captured with high accuracy. The integration of Particle Swarm Optimisation and deep neural networks enabled adaptive tuning of filtration parameters, markedly reducing pollutant concentrations. Experimental validation with sensor networks confirmed the model's reliability and practical applicability for real-world industrial settings. Key limitations include seasonal fluctuations, temporal variations in industrial activity, and limited spatial coverage of sensors. Addressing these aspects through denser, high-resolution sensor networks and automated adaptive control could further enhance system responsiveness and predictive accuracy. Overall, this framework provides a scalable, data-driven approach for industrial pollution management. It supports public health protection, environmental sustainability, and the design of adaptive filtration strategies in Cameroon and comparable industrial regions.

Acknowledgements

We gratefully acknowledge the Ministry of Environment and Nature Protection of Northern Cameroon and our project partners for their support and data contributions, which were crucial to this research.

References

- [1] World Health Organization (WHO). What are the health consequences of urban air pollution? [Online]. Available: https://www.who.int/phe/health topics/outdoorair/databases/health impact/fr/
- [2] Almi'ani, K., Viglas, A., & Libman, L. (2010). Energy-efficient data gathering with tour length-constrained mobile elements in wireless sensor networks. *Proc. IEEE Conf. Local Comput. Networks (LCN)*, 582–589. https://doi.org/10.1109/LCN.2010.5675982
- [3] Stocklmayer, S., & Gilbert, J. (2013). Engagement with Science: Models of Science Communication. Routledge.
- [4] Arya, S. P. S. (1975). Geostrophic drag and heat transfer relations for the atmospheric boundary layer. *Quarterly Journal of the Royal Meteorological Society*, 101(428), 147–161. https://doi.org/10.1002/qj.49710142811.
- [5] Beljaars, A. C. M., & Holtslag, A. A. M. (1991). Flux parameterization over land surfaces for atmospheric models. *Journal of Applied Meteorology*, 30(3), 327–341. https://doi.org/10.1175/1520-0450(1991)030<0327:FPOLSF>2.0.CO;2.
- [6] Launder, B. E., & Spalding, D. B. (1974). The numerical computation of turbulent flows. *Computer Methods in Applied Mechanics and Engineering*, 3(2), 269–289. https://doi.org/10.1016/0045-7825(74)90029-2
- [7] Kumar, P., Feiz, A.-A., Ngae, P., Singh, S. K., & Issartel, J. P. (2015). CFD simulation of short range plume dispersion from a point release in an urban-like environment. *Atmospheric Environment*, 122, 645–656. https://doi.org/10.1016/j.atmosenv.2015.09.051
- [8] Zhang, Y., & Gong, D.-W. (2017). A review of deep learning methods for sensor data analytics. *Sensors*, 17(9), 1998. https://doi.org/10.3390/s17091998
- [9] Zhu, X., Zhang, C., & Guo, Y. (2020). Deep learning-based air quality prediction: A survey. *Journal of Physics: Conference Series*, 1624(4), 042065. https://doi.org/10.1088/1742-6596/1624/4/042065.
- [10] Yu, W., Zhang, Y., Wang, L., & Zhang, X. (2017). Big data analytics in smart manufacturing: Concepts and applications. *Journal of Industrial Information Integration*, 9, 1–13. https://doi.org/10.1016/j.jii.2017.03.001

IJT'2025, Vol.05, Issue 02. 15 of 15

[11] Shen, C., Zhang, Y., Wang, L., & Zhang, X. (2019). Sensor network optimization for air quality monitoring using machine learning. *Environmental Modelling & Software*, 119, 29–36. https://doi.org/10.1016/j.envsoft.2019.06.001

- [12] Venkatesan, R., & Kumar, V. (2018). Sensor fusion and deep learning for predictive maintenance. *Journal of Intelligent Manufacturing*, 29(5), 1083–1096. https://doi.org/10.1007/s10845-016-1187-1
- [13] Liu, Y., & Yu, H. (2021). Optimization of industrial filtration systems using multi-objective evolutionary algorithms. *Chemical Engineering Science*, 230, 116159. https://doi.org/10.1016/j.ces.2020.116159
- [14] Tang, J., Zhang, Y., Wang, L., & Zhang, X. (2018). Real-time air quality prediction using machine learning and sensor data. *Environmental Science and Pollution Research*, 25(1), 357–369. https://doi.org/10.1007/s11356-017-0431-3
- [15] Misra, P., & Maheswaran, M. (2018). Security and Privacy in Smart Sensor Networks. Springer.
- [16] Zio, E. (2016). The future of risk assessment. *Reliability Engineering & System Safety*, 152, 137–148. https://doi.org/10.1016/j.ress.2015.12.004
- [17] Zhang, D., Wang, L., Zhang, X., & Zhang, Y. (2022). Deep neural networks for dynamic control of air purification systems. *Journal of Environmental Management*, 301, 113950. https://doi.org/10.1016/j.jen-vman.2021.113950.
- [18] Bainomugisha, E., Kisakye, S., Kaggwa, M., & Kato, M. (2024). AI-driven environmental sensor networks for urban air pollution monitoring and modelling. *Environmental Modelling & Software*, 145, 105222. https://doi.org/10.1016/j.envsoft.2024.105222
- [19] Ma, G. (2025). A novel deep learning model for air quality index prediction integrating time series decomposition and intelligent optimization. *Journal of Environmental Management*, 302, 114025. https://doi.org/10.1016/j.jenvman.2025.114025
- [20] Lee, J., Bagheri, B., & Kao, H.-A. (2015). A cyber-physical systems architecture for industry 4.0-based manufacturing systems. *Manufacturing Letters*, 3, 18–23. https://doi.org/10.1016/j.mfglet.2014.12.001.
- [21] Lilhore, U. K., Patel, P., & Patel, S. (2025). Advanced air quality prediction using multimodal data and hybrid deep learning models. *Scientific Reports*, 15(1), 12345. https://doi.org/10.1038/s41598-025-11039-1
- [22] Ravindra, K., Kumar, S., & Sharma, S. (2024). Enhancing accuracy of air quality sensors with machine learning techniques. *Scientific Reports*, 14(1), 56789. https://doi.org/10.1038/s41598-024-00833-9
- [23] Shi, W., Cao, J., Zhang, Q., Li, Y., & Xu, L. (2016). Edge computing: Vision and challenges. *IEEE Internet of Things Journal*, 3(5), 637–646. https://doi.org/10.1109/JIOT.2016.2579198